Controlled Planar Alignment of Discotic Liquid Crystals in Microchannels Made Using SU8 Photoresist

James Cattle, Peng Bao, Jonathan P. Bramble, Richard J. Bushby, Stephen D. Evans, John E. Lydon, and Daniel J. Tate*

A range of triphenylene and phthalocyanine-based discotic liquid crystals (DLCs) can be aligned within micrometer-scale channels formed from SU8 patterned on silicon or glass surfaces. The channels can be filled with the DLC in its isotropic phase using capillary action. Alignment occurs spontaneously as the sample is slowly cooled into the Col_h phase. Whilst all of these DLCs align with the columns perpendicular to the surface when they are 'sandwiched' between glass slides, in these channels, the DLC aligns with the column director parallel to the surface. It is also constrained to lie across the channels. The same alignment occurs when these DLCs are confined between SU8-topped interdigitated gold electrodes where it gives the optimum orientation for electrode-to-electrode conduction. The quality of the alignment depends on the particular liquid crystal used and on the width of the channel. For the Col_r phase of octaoctylphthalocyanine there is additional epitaxial control over the orientation of the lattice such that the a/c face of the lattice is parallel to the surface. This is an important prerequisite for creating a bistable display device that switches by virtue of changing the direction of the tilt of the discs.

1. Introduction

Commercial applications of discotic liquid crystals (DLCs) such as the manufacture of optical compensating films[1,2] and the production of carbon fibers[3–5] rely on the ease with which nematic phases of DLCs can be aligned. Development of future applications such as field effect transistors[2,6–12] and photovoltaic devices[2,13–16] depend on solving the much more difficult problem of how to control the alignment of columnar phases. For DLCs, nematic phases are actually rather rare. In the vast majority of cases, cooling of the isotropic melt leads directly into a columnar phase. In these cases, the techniques that are currently used to align nematics are ineffective. Columnar phases of DLCs are remarkably insensitive to surface chemistry or roughness.[17,18] Almost universally, they adopt a homeotropic alignment at the solid-to-liquid crystal interface and a planar orientation at the air-to-liquid crystal interface. When thin films that are open to the air are slowly cooled there is often a conflict between the preferred alignment at the air-to-liquid crystal interface and that at the solid-to-liquid crystal interface. But, if the films are very thin and cooling is slow or if they are annealed just below the columnar-isotropic transition temperature, it is the stronger anchoring at the air interface that usually dominates.[19,20] As a result, columnar phases that align in a homeotropic manner when sandwiched between glass slides or between ITO electrodes align in a planar fashion in thin 'open-to-the-air' films. In such films there is normally a distribution of the column directors within the plane of the substrate (samples are described as 'random planar') but a number of ways have been developed of preparing 'uniaxial planar' samples (samples where all of the columns are aligned parallel to the substrate and all of them point in the same direction). Spin-coating[21] or shearing samples[22] can sometimes achieve such uniaxial alignment but more generally reliable methods are Langmuir–Blodget deposition,[23] the use of PTFE-rubbed substrates,[23–27] zone-casting,[12,23,28–31] zone-melting[32] and alignment within channels.[33,34] 'Uniaxial planar' samples are essential for making electronic devices such as field effect transisitors where it is important to ensure that the column direction, the preferred axis for conduction, runs in-plane from source to drain electrode.

Very thin open films of DLCs have a tendency to dewet from the surface: particularly when they are heated into the isotropic phase. On a surface patterned with alternating high and low energy stripes this dewetting produces long thin droplets (as shown schematically in cross-section in **Figure 1**a). This not only enforces a planar alignment of the column director but also provides control over its in-plane orientation.[35] For some liquid crystals it lies across the droplets and in others parallel to their long axis. In this paper we show that the same sort of control can also be achieved for a range of DLCs

J. Cattle, Prof. R. J. Bushby, Dr. D. J. Tate
School of Chemistry
University of Leeds
Leeds, LS2 9JT, UK
E-mail: R.J.Bushby@leeds.ac.uk
Dr. P. Bao, Dr. J. P. Bramble, Prof. S. D. Evans
School of Physics and Astronomy
University of Leeds
Leeds, LS2 9JT, UK
Dr. J. E. Lydon
Faculty of Biological Sciences
University of Leeds
Leeds, LS2 9JT, UK

DOI: 10.1002/adfm.201301613

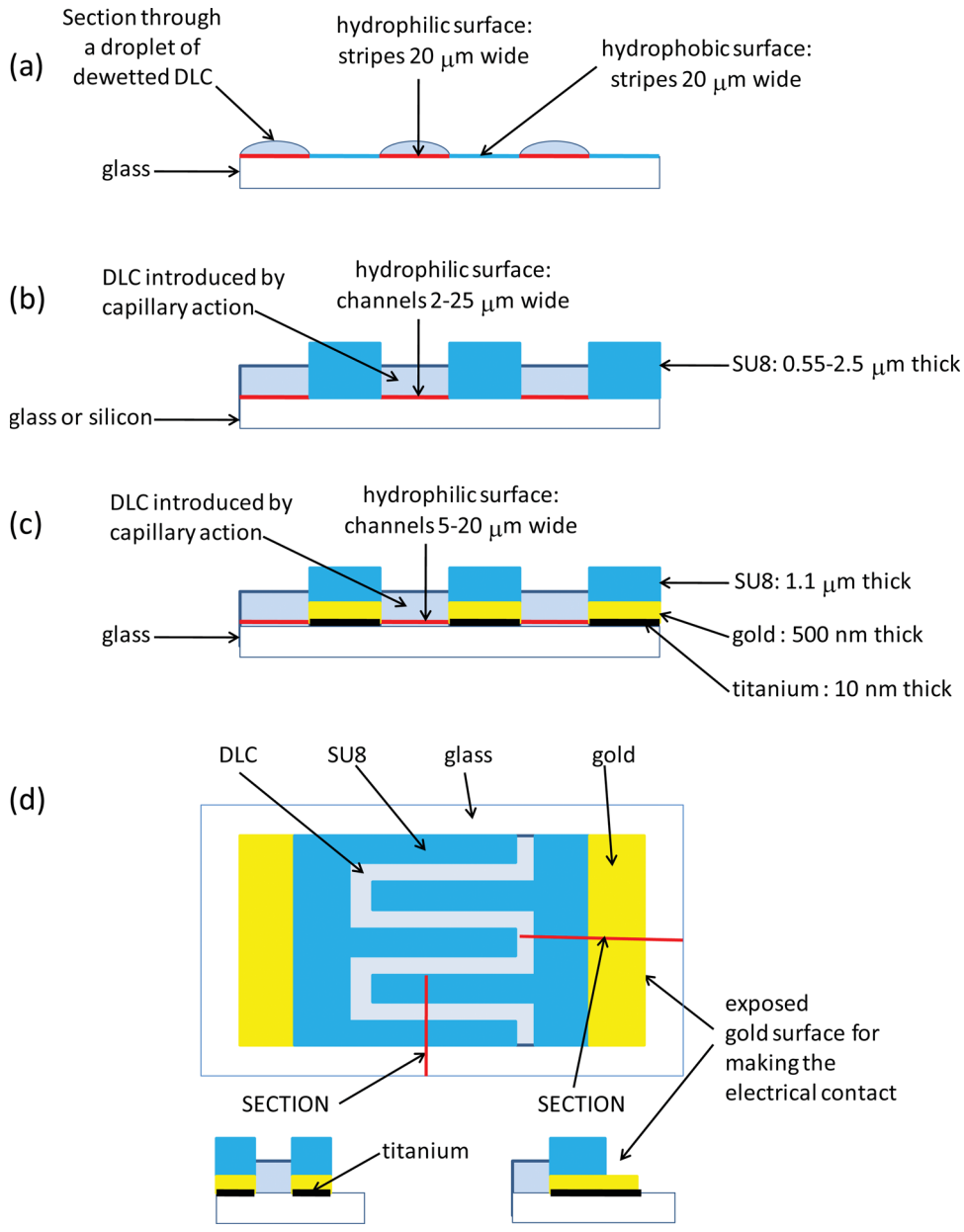

Figure 1. Schematic representation of the various systems discussed in this paper. a) Dewetting method: Cross-section perpendicular to the long thin 'dewetted droplets'. b) Cross-section of the DLC aligned in SU8 microchannels. c) Cross-section of the DLC aligned between interdigitated SU8 capped gold electrodes. d) Plan view of the interdigitated electrodes showing how the electrical contacts were made. For the sake of clarity only five electrodes are shown. In reality there were many.

using thin open films constrained within microchannels fabricated from SU8 photoresist on glass or silicon substrates. Compared to the 'dewetted droplet' systems (Figure 1a)[35] the hydrophobic SAM is replaced by SU8 (Figure 1b) or SU8-capped gold (Figure 1c,d). (SU8 is an epoxy side-chain substituted poly(methylenephenylene) which cross-links under UV irradiation and as such is relatively hydrophobic.) The main precedent for such alignment in channels is the report of the alignment of the columnar phases of a phthalocyanine-based DLC in SiO_2 nanoscale channels due to Mouthuy et al.[33,34] These nanometer-scale channels were fabricated using E-beam lithography and were filled by spin-coating. However, for these it was concluded that alignment was confined to substrates patterned on the sub-micrometer scale.[34] The SU8 micrometer-scale channels described in the present paper are much easier to make and they can be filled by a much simpler method: simply by capillary action.[36,37] We also show that alignment can be achieved using SU8 channels which are up to 25 μm wide and that this approach is applicable to a whole range of DLCs with both triphenylene and phthalocyanine nuclei but, in particular, the alignment between SU8 capped electrodes and the additional control over the alignment found in the case of the Col_r phase are potentially important in terms of future applications.

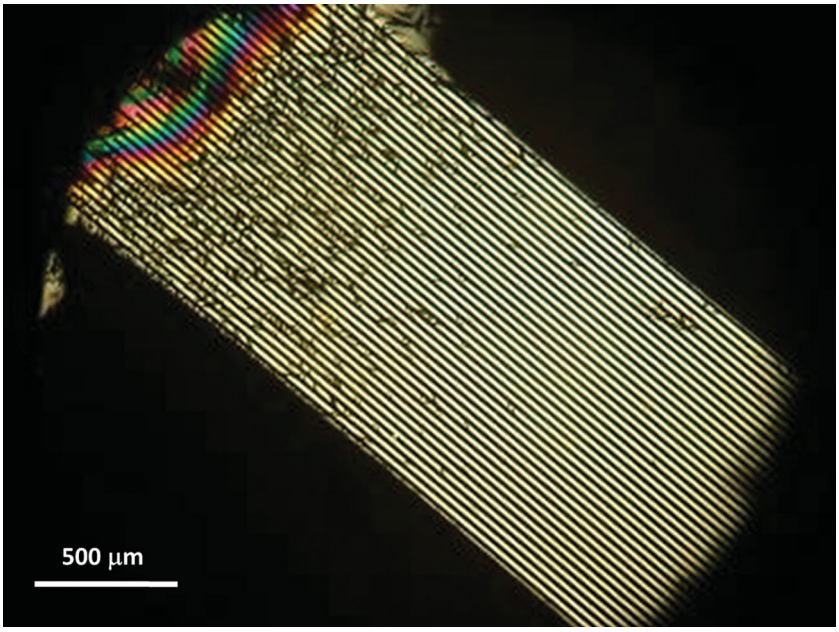

Figure 2. Transmission mode POM image of HHTT **1** filled by capillary action in the isotropic phase into 10 μm wide channels. The barriers are made of SU8 and are 0.55 μm high and 10 μm wide and the substrate is glass. To generate this image liquid crystal was cooled quite rapidly (0.5 °C/min) into the Col_h phase (≈85 °C). Slower cooling (0.1 °C/min) removes most of the defects. Image taken with the channels at 45° to crossed polarizers.

2. Results and Discussion

2.1. Filling of SU8 Microchannels and Alignment of the DLC

Figure 2 shows a POM image of a glass slide patterned with SU8 barriers separated by 10 μm wide channels. A small crystalline sample of HHTT **1** has been added (top left) and the DLC heated into its isotropic phase when the melted liquid rapidly and spontaneously filled into the channels. This capillary filling of the channels is presumably so efficient because the glass/SiO_2 provides a high energy surface at the bottom of each channel. The sample has been cooled at 0.5 °C/min into its Col_h phase, the channels are at 45° to crossed polarizers and the microscope is in transmission mode. Over most of the sample, the Col_h liquid crystal is aligned and it is the expected 'first order grey'. When, as in this case, the sample is cooled unusually rapidly there are some alignment defects within the channels: particularly close to the source (top left) where the sample is thickest. The number of such defects depends on the rate at which the sample is cooled. As shown in the other images in this paper and in the supporting information, a slower cooling rate of 0.1 °C/min eliminates almost all of the defects. The colored birefringent region at the top left of Figure 2 is due to overfilled channels. Furthest away from this source (bottom right of Figure 2) either the channels are unfilled or the liquid crystal sample is so thin that the birefringence can no longer be detected. Hence the depth of the liquid crystal in the channels must decrease from top left to bottom right of the Figure. This was confirmed by tapping mode AFM studies of H7T filled, into 2 μm wide channels (H7T supercools, remaining in its Col_h phase down to room temperature). Very close to the source of the liquid crystal AFM showed that there is a height difference between the surface of the SU8 and the surface of the liquid crystal of about 60 nm which implies a depth of liquid crystal in the channel of ca. 490 nm. At ≈2 mm further down the channel this height difference was about 175 nm corresponding to a depth of liquid crystal in the channels of about 275 nm and another ≈2 mm further down (at a point where POM suggests that the channel is empty or almost empty) the height difference was 550 nm: essentially the thickness of the SU8 as measured by the profilometer (0.55 μm). Further details of these AFM studies are given in the supporting information.

When a well-aligned sample of a DLC in its Col_h phase is viewed using POM and crossed polarizers and with the channels at 0° or 90° the image becomes wholly black. Assuming the columns are aligned in-plane, this indicates that they are oriented either along or perpendicular to the channels.

2.2. Orientation of the Director in Col_h DLC Systems

In our earlier work on the orientation of the director in dewetted droplets,[35] we distinguished between situations in which the director was aligned along the channels and those in which it was oriented perpendicular to the channels by using a mixture of POM (the changes induced in the birefringence colors by introducing a 1λ wave plate) and GISAXS (grazing-incidence small-angle X-ray scattering). In the case of the SU8 microchannels, there is too much X-ray scattering from the SU8 for GISAXS to reveal the orientation of the column director. As a result we are wholly dependent on POM. However, since the DLCs are mostly the same as those which we used before and, since our previous POM results were correlated with the GISAXS results, in the present case POM can be used on its own. To further strengthen the evidence, we have also calculated the expected changes in birefringence color as a function of sample thickness, orientation and birefringence and as a function of the alignment of the 1λ wave plate. Details of these calculations are given in the supporting information. They show that, for a typical columnar phase with a birefringence of 0.12 and with a maximum thickness of ≈1.1 μm for transmission mode experiments (on glass substrates) and ≈5 μm (2 × ≈2.5 μm) for reflection mode experiments on silicon substrates we should observe 'first order grey' in most cases shading into orange/red for the very longest pathlengths. This is what we observed experimentally. The calculations further showed (as expected) that, for a 'first-order grey' sample when the 1λ wave plate is added with its slow axis orthogonal to the slow axis of the sample, it should appear as second-order yellow/orange and when these are aligned parallel the sample should appear as second-order blue.

Figure 3 shows a typical set of POM results. In this case HHTT **1** has been aligned in 25 μm wide channels on silicon. The sample is in the Col_h phase at 85 °C and the microscope used in reflection

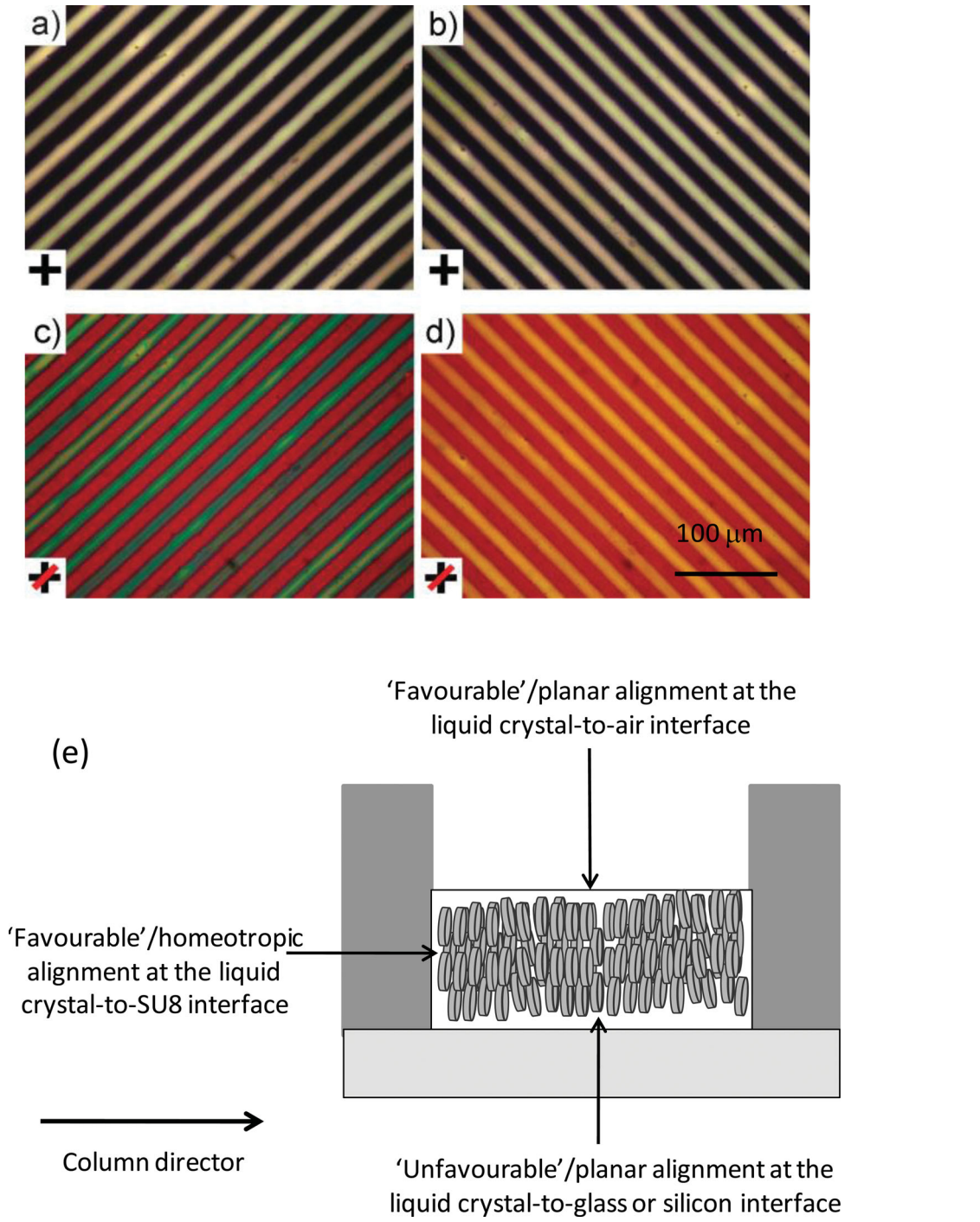

Figure 3. a–d) Reflection mode POM images of HHTT 'filled' by capillary action in the isotropic phase into 25 μm wide × 2.5 μm deep SU8 channels on silicon and cooled slowly (0.1 °C/min) into the Col_h phase (85 °C). The images were taken with the channels at ±45° to crossed polarizers. a,b) Without the 1λ wave plate. c,d) With the 1λ wave plate in place. The red line indicates the orientation of the slow axis of the compensator. e) Schematic representation (not to scale) of a Col_h phase aligned across the channels.

mode with the channels at ± 45° to crossed polarizers. In the top images a and b, since the sample is thin, the DLC is mainly first order grey. The two lower images c and d are the same areas of the wafer as those shown at the top also under crossed polarizers but with the addition of a 530 nm 1λ compensator plate oriented with its slow axis in the direction shown by the red line. The addition of the wave plate makes the SU8 appear to be red and the DLC, which was close to 'first order grey', appears blue/green when the slow axis of the wave plate is aligned with the channels and yellow when they are at 90° to each other. These color differences unambiguously indicate that the column director lies across the channels. The same result was obtained for HHTT on glass substrates

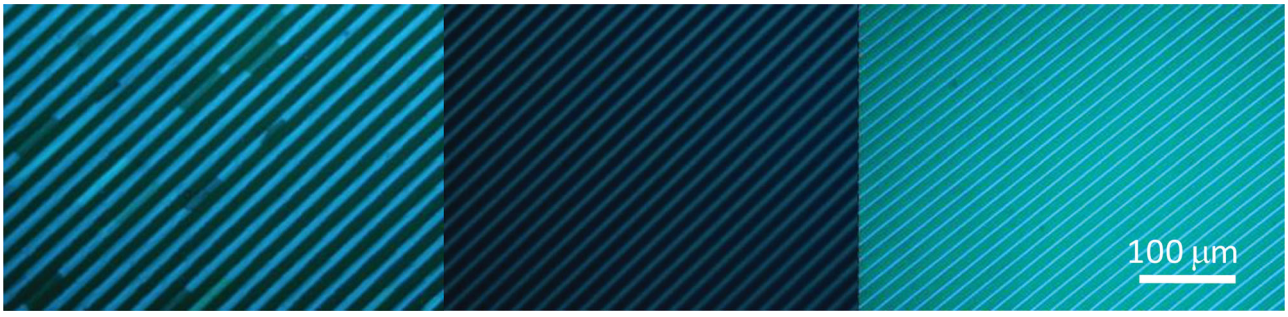

Figure 4. POM images of i7H_2Pc **7** in SU8 microchannels on silicon at 140 °C (Col$_h$ phase). Channel widths are (from left to right) 10 μm, 5 μm, and 2 μm. The microscope is in reflection mode.

(i.e., in transmission mode experiments) and for HAT6 **2**, for H7T **3** and the 'acrylate monomer' **4** (as shown in the supporting information). In each case the column director is oriented across the channels. Compared to the results obtained for long thin droplets of the Col$_h$ phase the orientation of the director for HAT6 and H7T is the same but for HHTT it is different. In the dewetted droplets the HHTT aligns with the director along the axis of the droplet.

For the three phthalocyanines **5–7**, aligned samples extinguished the light when the channels were oriented at 0° or 90° relative to crossed polarizers and so, again assuming planar alignment, the column director either lies along or across the channels. Their strong absorption in the visible region of the spectrum made it impossible to distinguish between these two possibilities using the 1λ wave plate. Most probably, they align with the director across the channels since this gives a homeotropic alignment with the surface of the SU8 (Figure 3e).

2.3. The Effect of the Width of the Channel on the Alignment of the DLC

Alignment with the column director in-plane and across the channels gives the favorable 'planar' orientation of the director at the liquid crystal-to-air interface, a favorable homeotropic alignment at the SU8 walls but an unfavorable planar alignment at the glass-to-liquid crystal (or silicon-to-liquid crystal) interface as shown schematically in Figure 3e. This suggests firstly that anchoring at the air interface is the stronger than that on glass (or oxide-coated silicon) and secondly that alignment across rather than along the channels is dictated by preferred homeotropic anchoring on the SU8.

For films sandwiched between two solid substrates it is found that it is usually easiest to align very thin films and, as the thickness of the film is increased, either the samples have to be cooled much more slowly or they have to be annealed for many hours just below the Col-I transition temperature. Indeed it is often impossible to fully align samples if they are thicker than a few tens of micrometers. Hence, if in the present instance, the alignment across the channels is dictated by homeotropic anchoring at the SU8 interface, the ease of this alignment should depend on the width of the channel. It should also depend on the molecular structure of the DLC since this is a major factor in determining the strength of the anchoring interactions. This proves to be the case.

Figure 4 shows a set of three images that were acquired for i7H_2Pc **7** in different size microchannels on silicon wafers (channels 2, 5, and 10 μm wide and 2.5 μm deep). In each case a standard cooling rate of 0.1 °C/min was employed There is good alignment in channels that are 2 and 5 μm wide but in those that are 10 μm wide there are some misaligned regions. These experiments were repeated with the same cooling rate for all of the DLCs shown in **Scheme 1** and the results are

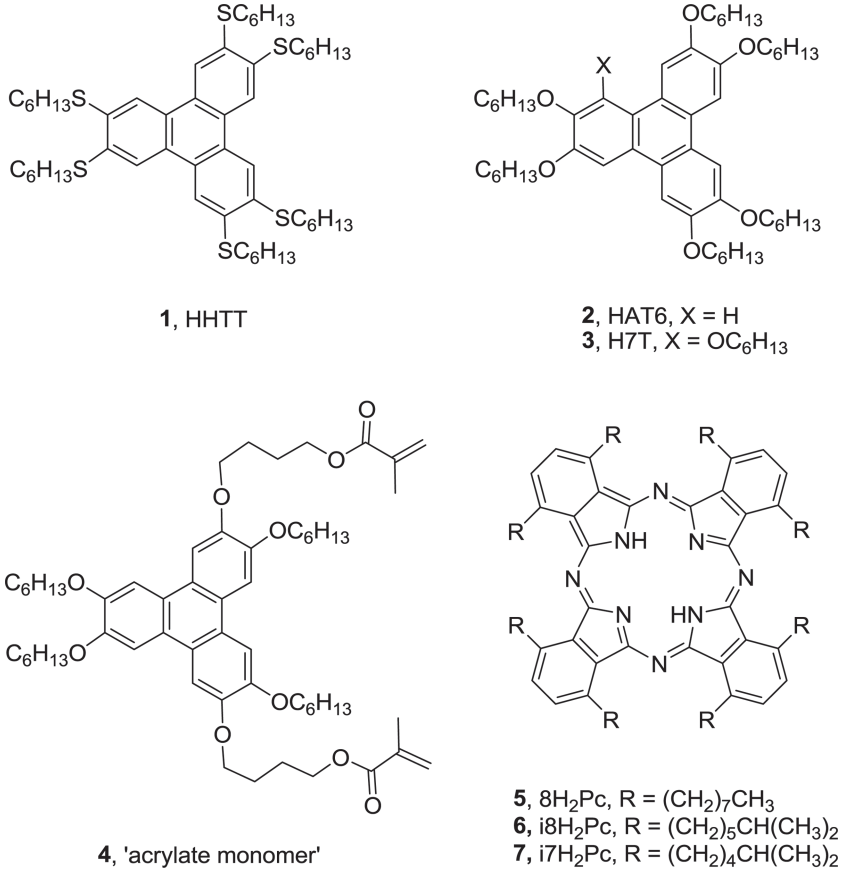

Scheme 1. Molecular formulae of the DLCs used in this study.

Table 1. Results of attempts to align the DLCs between 2.5 µm high SU8 barriers in channels which were 2 µm, 5 µm or 10 µm wide on a silicon substrate. In each case the experiment was conducted in exactly the same way and the sample was cooled from the isotropic phase at a rate of 0.1 °C/min. The actual images are shown in Figure 4 and in the supporting information. For HHTT **1**, good alignment was also obtained in 25 µm wide channels (Figure 3).

DLC	10 µm	5 µm	2 µm
HHTT 1	YES	YES	YES
HAT-6 2	YES	YES	YES
H7T 3	NO	YES	YES
'acrylate monomer' 4	NO	YES	YES
$8H_2Pc$ 5	NO	YES	YES
$i8H_2Pc$ 6	NO	NO	NO
$i7H_2Pc$ 7	NO	YES	YES
Aspect Ratio	**4:1**	**2:1**	**0.8:1**

summarized in **Table 1**. The POM images are given in the supporting information.

From the results shown in Table 1, it is clear that, as expected, it is easier to align the liquid crystals in the narrower channels but that the ease of alignment also depends on the molecular structure of the discogen. Some of these effects are very subtle. The difference between $8H_2Pc$ and $i8H_2Pc$ is only in the terminal part of the disordered side-chains but the alignment behavior is quite different!

2.4. Alignment of the Col_r phase of $8H_2Pc$ 5

The phthalocyanine $8H_2Pc$ **5** provides a particularly interesting case since it forms not only a Col_h phase, where a single director, the column director n^z, has to be considered, but also a Col_r phase, where two directors needs to be considered, n^z (relating to the orientation of the columns) and n^x (relating to the orientation of the lattice perpendicular to the columns). When the Col_h phase of $8H_2Pc$ 5 is aligned in SU8 microchannels and is viewed with the channels at 0 or 90° relative to crossed polarizers it is fully black. The column director and the unique optic axis (or at least the projection of the optic axis) are aligned with the polarizers - almost certainly in-plane with the columns lying across the channels. When the sample is cooled below 101 °C (the point at which the rectangular columnar Col_r phase is formed) the image suddenly becomes bright (**Figure 5**a). Close examination shows that the liquid crystal is now crossed by many grain boundaries. Adding a wave plate shows that these delineate two (and only two) different domain types (Figure 5d). The wave plate reveals two differently colored areas - some maroon and the others pale blue. These domains

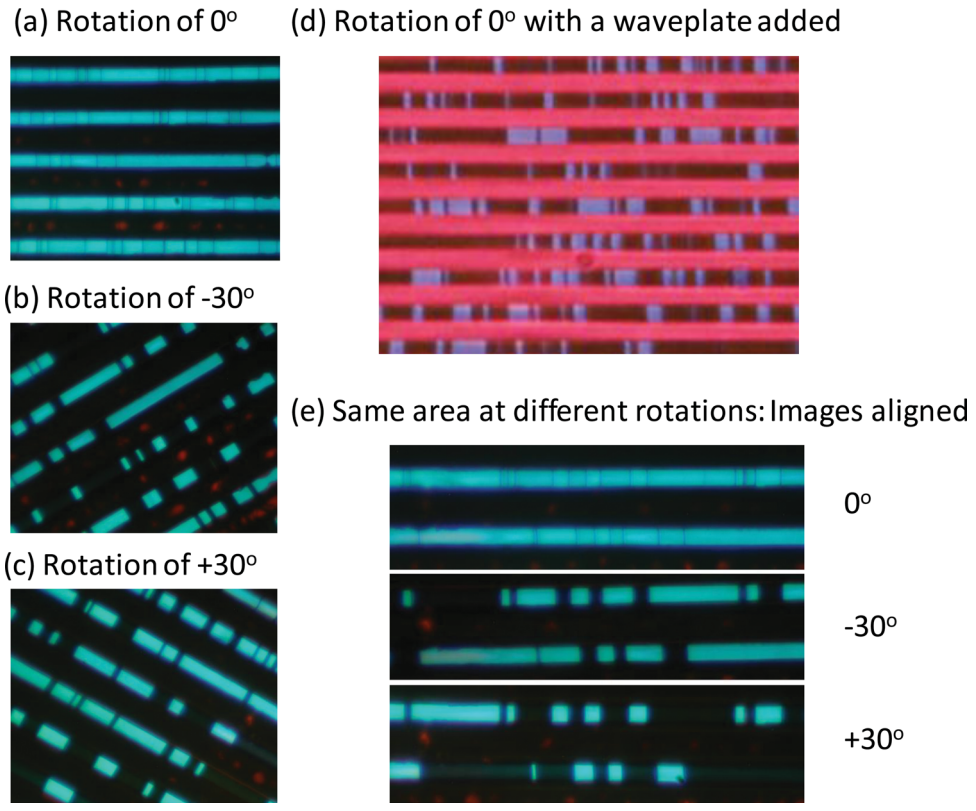

Figure 5. $8H_2Pc$ **5** in the Col_r phase at 80 °C aligned in 5-µm-wide microchannels on glass. Images taken in transmission mode using crossed polarizers a) with the channels aligned with one of the polarizers (0°) and b,c) then rotated by ±30°. This gave the maximum extinction values. d) The effect at 0° rotation of adding the wave plate. e) The aligned regions of the same two stripes presented one above the other showing that, between the limits of +30° and −30° the blue areas become black and vice versa.

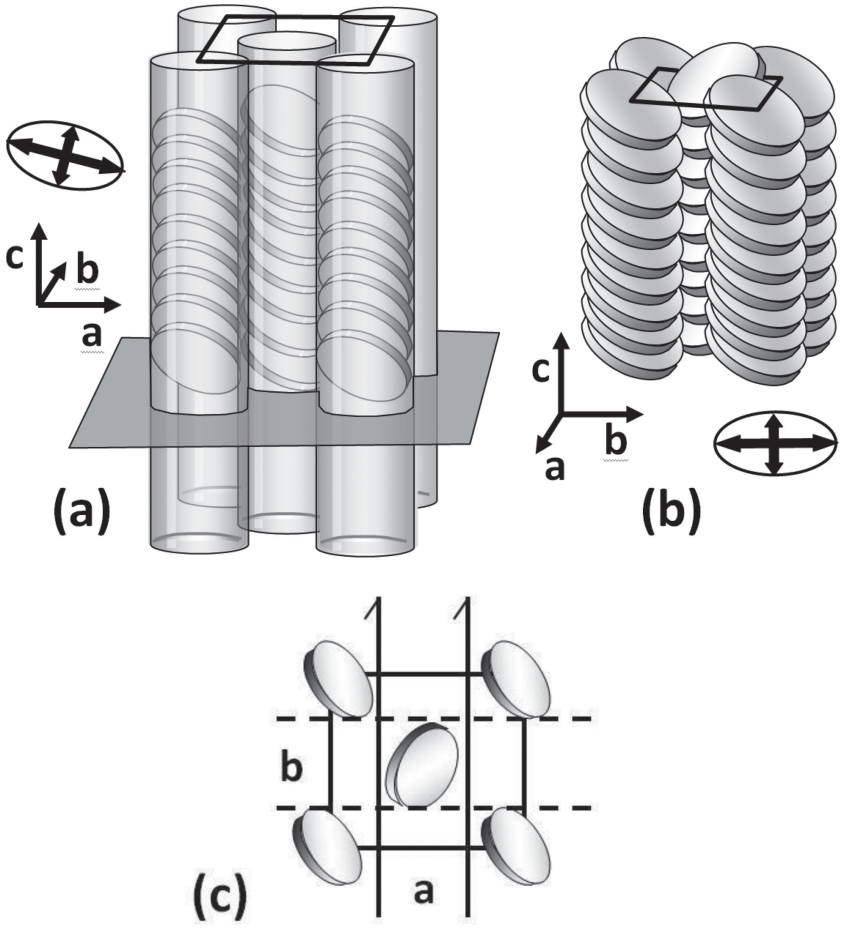

Figure 6. Schematic representation of the Col_r ($P2_1/a$) phase. a) Perspective view along the b-axis (with the a/c face parallel to the surface). b) Perspective view down the a-axis (with the b/c face parallel to the surface). c) Unit cell/view down the column axis. The two-fold screw axes are shown as single-headed arrows and the glide planes as dashed lines. Note that, although this schematic represents the orientation of the molecules, it does not imply correlation of their positions along the columns. In reality there is none. The bold, crossed, double-headed arrows drawn within ellipses represent the principal axes of the biaxial indicatrix as viewed perpendicular to the a/c or b/c plane. Note that, in the projection shown in (a), all of the molecules slope downwards from upper left to lower right. This causes the major axes of the projection of the indicatrix to be offset at an angle to the crystallographic axes.

involve opposite orientations of the optic axes. Hence, when (with the wave plate removed) the sample is rotated in an anticlockwise sense by −30° (Figure 5b) half of the domains delineated by the grain boundaries become black and, when rotated in a clockwise sense by +30° (Figure 5c), the colors are reversed. This is perhaps easiest to see in Figure 5e where the same regions for the same channels are lined up and presented one-above-the-other. This behavior is what is expected if the orientations of *both* n^z and n^x are controlled and if (but only if) the sample is uniaxial planar and n^x is oriented such that the a/c face of the lattice is parallel to the surface.[38,39] In the Col_h phase, (on average)[40] the discs are perpendicular to the column axis, the columns have an effectively circular cross-section and the column axis and the unique optic axis are coincident. However, in the Col_r phase this is no longer true. There is a correlated tilt of the discs[40] and the optic axes are now at an angle to the column.[38,39] For this phthalocyanine the Col_r phase is probably ($P2_1/a$) [although diffraction studies were unable to exclude the alternative that it is of the much rarer (P2/a) type].[41] The case for ($P2_1/a$) is analyzed here and the almost identical case for (P2/a) is analyzed in the supporting information. The unit cell for Col_r ($P2_1/a$) is shown in **Figure 6**c. When this is viewed along the b axis (viewed parallel to the two-fold screw axis of the unit cell or with the a/c plane parallel to the surface in the POM experiments) the molecules within the columns all slant in the same direction (top left to bottom right) and, in the example illustrated, the (projected) optic axes of the sample are rotated in a clockwise sense (Figure 6a). There is, however, an equally probable, equal energetic state in which the discs tilt in the opposite direction and the (projected) optic axes are rotated in an anticlockwise sense.[38,39,42] It is this that gives rise to the two domains, one of which extinguishes at a rotation of +30° and the other at a rotation of −30°.[39,40] When the unit cell for the Col_r ($P2_1/a$) phase is viewed along the a axis (viewed parallel to a glide plane of the unit cell or viewed with the b/c plane parallel to the surface in a POM experiment) there is an equal number of columns (per unit cell) in which the molecules slant to the left and to the right (Figure 6b). In such a case the (projected) optic axes of the whole sample will appear to be unchanged relative to the Col_h phase and will be appear to be the same for both domains. In Figure 5a,d domains of this type would be black; but, over the whole sample, no such regions could be found. This argument is true for any type of Col_r phase since (by convention) the mirror/glide planes of the unit cell are parallel to the a/c plane and the two-fold screw/rotational axes are parallel to the b axis. A fuller, discussion of the relationship between the liquid crystal lattice and the optical properties of oriented DLC films, including an analysis for other Col_r phases, is given in the supporting information.

An interesting consequence of this particular type of alignment is that it affords the prospect of designing a display device that switches by virtue of changing the direction of tilt of discs within the columns of a Col_r phase. Such a device would be the direct DLC analogue of bistable, fast-switching chiral calamitic smectic C devices which rely on manipulating the direction of tilt of rod-like molecules with the smectic layers.[43,44] In particular, note that in a Col_r phase with the a/c face parallel to the surface there are glide or mirror planes parallel to the surface and the screw/rotational axes are perpendicular to the surface and this is exactly analogous to the symmetry properties exploited in smectic C devices. Although there are a number of ways in which a ferroelectric response can be introduced into the Col_r phase,[45–50] given the analogy to the smectic C

systems, the obvious choice is to do this in the same manner. Introducing polar homochiral side-chains would lift the mirror plane symmetry and give a net dipole perpendicular to the surface.[43–44] This idea has previously been forwarded by Scherowsky and Chen[22] who demonstrated that for an (essentially) unoriented Col_r mixture of phenanthrene-based DLCs with homochiral polar side-chains switching times are of the order 10^{-2} s. The prospect now exists of creating samples that have the ideal orientation for this type of switching.

This kind of epitaxial control over the orientation of the lattice perpendicular to the column axis is known for some columnar phases (for example those of bolaamphiphiles)[51–52] but it is not seen in all thin films of columnar phases of DLCs. Hence, in drop-cast open films of benzene-based DLCs[39] and triphenylene-based DLCs[38] with Col_r ($P2_1/a$) phases what is observed is a mixture of domains in some of which the a/c face is parallel to the surface (the optic axes are rotated to the left and to the right) while in others the b/c face is parallel to the surface (the optic axes appear to be unchanged relative to the Col_h phase). That is, there is only partial control over the orientation of n^x. However, full epitaxial control is probably not specific to this method of alignment in microchannels or to this particular DLC. Note that very similar optical effects to those described in this paper were reported for dewetted droplets of the Col_r phase of $8H_2Pc$, (see Figure 5a of ref. [35]). Also note that GISAX studies of dewetted droplets of the Col_h phases of HHTT 1, H7T 3 and $8H_2Pc$ 5, show a preference for the {10} plane of the lattice to lie parallel to the surface.[35]

2.5. Alignment of DLCs Between SU8-capped Interdigitated Electrodes

As well as being aligned between SU8 channels, these DLCs can also be aligned between SU8-capped gold electrodes which enables their conductivity to be addressed. POM studies of these samples showed the DLCs to be well aligned and black when viewed with the channels parallel to one of a pair of crossed polaizers. It is important to emphasize that these electrodes need to be SU8-capped. When interdigitated gold electrodes are used that are not coated with SU8, there is no capillary filling. In this case, when drop-cast thin films of the DLCs are heated into the isotropic phase, they wet both the top of the electrodes and the space between the electrodes and no overall alignment is achieved. **Figure 7** shows the I/V response obtained for HHTT filled SU8 capped interdigitated gold electrodes using a voltage sweep of ±30 V for the Col_h phase and for the isotropic phase. As shown, the conductivity is dependent on the phase of the DLC. The current is very small but it is of the same order as that obtained for homeotropically aligned DLCs sandwiched between 10 μm × 10 μm ITO electrodes at a separation of 6 μm.[53] In both cases the 'exposed' area of the electrodes is estimated to be about 100 μm^2 and the current is space-charge limited.[53] However, in the case of these interdigitated electrodes, as compared to 'sandwich cell' samples there is more hysteresis in the *I–V* response suggesting that there is ppm ionic contamination. Possibly this ion-contamination has arisen from ions adsorbed on the surface during the wet etching process that we have not been able to remove. These results demonstrate the principle of spontaneous uniaxial planar alignment between pre-patterned electrodes. In the past, in making DLC based OFETs, it has been necessary to evaporate the source and drain electrodes on top of a pre-formed uniaxial planar DLC.[12,21,26]

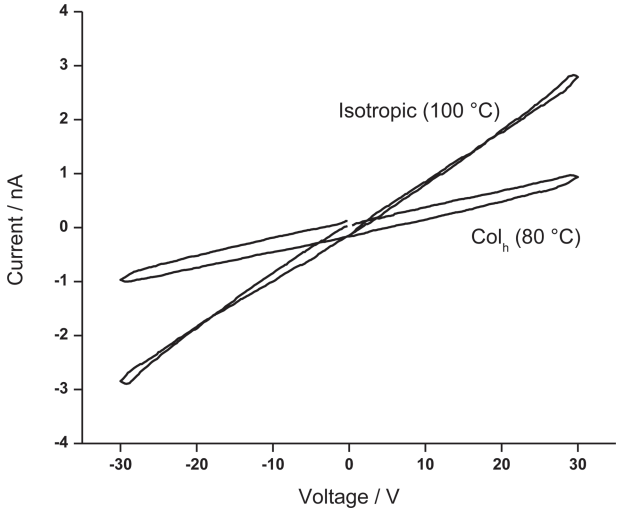

Figure 7. I/V response for HHTT confined and aligned between SU8-topped interdigitated gold electrodes in the isotropic phase (100 °C) and Col_h phase (80 °C). The separation between the electrodes is 5 μm. There was no detectable current before the DLC was introduced.

3. Conclusions

The previous work on alignment of columnar phases of DLCs in channels by Jonas et al exploited a single phthalocyanine-based DLC in nanoscale channels (<1-μm wide) which were fabricated by E-beam lithography on a silicon substrate and were filled by spin-coating. We have shown that a range of triphenylene and phthalocyanine DLCs can be aligned in micron-scale channels (up to 25-μm wide) created using SU8 and filled by capillary action: a much simpler procedure. We show that the alignment of the DLC requires slow (0.1 °C/min) cooling from the isotropic phase and that the alignment depends on the particular liquid crystal used and on the width of the channel (the distance over which the alignment effect needs to propagate and the strength of the anchoring interaction). In all cases, in which we have been able to check, the column director lies in-plane and across the channels. This is an alignment of the director that is favorable at the air interface and at the SU8 surface but not at the DLC/substrate interface. In the case of alignment between SU8-topped gold electrodes this means that the preferred conduction pathway runs from electrode-to-electrode and that this arises spontaneously so that it should be possible, for example, to fabricate FET structures in which the DLC is added to a pre-formed substrate rather than having to evaporate electrodes on top of a preformed 'uniaxial planar' DLC.[12,21,26] The alignment of the Col_r phase of $8H_2Pc$ is particularly interesting since it shows that, the orientation of both directors (n^z and n^x) is controlled. In symmetry terms, the orientation of the phase is the direct equivalent of that exploited

in bistable, fast-switching smectic C devices. As in these, the introduction of homochiral polar side-chains should result in a switchable system that relies on manipulating the direction of tilt of the discs. Related work by Scherowsky and Chen[22] suggests potential switching times of the order of 10^{-2} s. It is important to note that, to do this effectively, the orientation of both n^z and n^x need to be controlled. Other methods of producing 'uniaxial planar' columnar DLCs may only control (have only been reported to control) n^z.[38,39]

4. Experimental Section

Materials: HHTT **1**,[54] HAT-6 **2**,[55] H7T **3**,[35,56] 8H_2Pc **5**,[41,57] i8H_2Pc **6** and i7H_2Pc, **7**[58] were prepared according to published procedures. Spectroscopic, phase and analytical data was consistent with that reported. The molecular formulae are shown in Scheme 1. The synthesis and characterization of the 'acrylate monomer' are detailed in the supporting information. The phase behavior of these liquid crystals was as follows: **1**, HHTT: Cr 62 °C H 70 °C Col_h 93 °C I. **2**, HAT6: Cr 70 °C Col_h 100 °C I. **3**, H7T: Cr 44 °C Col_h 71 °C I. **4**, 'acrylate monomer': Cr 64 °C I 55 °C Col_h 38 °C Cr. **5**, 8H_2Pc: Cr 85 °C Col_r 101 °C Col_h 152 °C I. **6**, i8H_2Pc: Cr 124 °C Col_h 170 °C I 162 °C Col_h 20 °C Cr. **7**, i7H_2Pc: Cr 169 °C Col_h 189 °C I 169 °C Col_h 161 °C M 140 °C Cr. Except for the 'acrylate monomer' all of these DLCs were enantiotropic. All other chemicals were purchased from Sigma Aldrich and were used as received. SU8 was purchased from Chestech Ltd, UK. Silicon wafers were purchased from Si-Mat, Germany. High-purity gold was supplied by Goodfellow, UK

Fabrication of SU8 Microchannels on Silicon Wafers: All processing of SU8 microchannels was carried out under cleanroom conditions. Silicon wafers with dimensions 15 mm × 15 mm × 0.5 mm were ultrasonicated for 5 min each in acetone, isopropanol and deionized water. The wafers were cleaned with a 'pirahna' solution (70% H_2SO_4, 30% H_2O_2) for 10 min, rinsed in water and then dried under a stream of nitrogen. SU8 2002 was spin-coated onto the wafers. The thickness of the resist layer was controlled by varying the spin-speed. A 'soft bake' was carried out at 95 °C for 2 min followed by a slow cooling down to RT. A Karl Suss mask aligner was used to expose the resist with a dose of 30 mJ/cm^2. A post exposure bake of the SU8 was carried out at 95 °C for 2 min followed a slow cooling down to RT. After post-baking, a shallow pattern could be observed on the surface of SU8. The samples were developed for 2 min in EC Solvent (Chestech), followed by rinsing in isopropanol for 1 min and drying with nitrogen. The channels made by this method were ≈2.5 μm ≈1.1 μm or ≈0.55 μm deep and had channel widths of 2 μm, 5 μm, 10 μm, 20 μm and 25 μm (Figure 1b). The thickness of the SU8 films was measured using a KLA Tencor Profilometer.

Fabrication of SU8 Microchannels on Glass Slides: Microchannels with stripes defined by thinner SU8 layers were formed on glass substrates with dimensions 22 mm × 26 mm × 0.15 mm. The fabrication process was similar to that on silicon wafers. However, the exposure dose was slightly different: about 25 mJ/cm^2. Glass plates with ≈1.1 μm and ≈0.55 μm deep SU8 channels were produced by this method, with 2 μm, 5 μm and 10 μm wide channels (Figure 1b).

Fabrication of SU8 Coated Interdigitated Electrodes: For the purpose of performing electrical measurement on the ordered liquid crystal formed in the channels we made interdigitated gold electrodes capped with SU8. The interdigitated electrode pattern is shown schematically in Figure 1d. The structures were made on glass plates with dimensions 22 mm × 26 mm × 0.15 mm. The glass plates were cleaned in acetone, IPA, and piranha as before. They were baked on a hot-plate at 150 °C for 1 min before a layer of Au (≈500 nm) was deposited on top of a 10 nm Ti adhesion layer. An SU8 layer was spin-coated onto the Au. The sample was prebaked at 95 °C for 2 min followed a slow cooling down to RT. The exposure dose for the SU8 was only 5 mJ/cm^2: much lower than that for glass or silicon wafers. The samples underwent a post-baking at 95 °C for 2 min followed by a slow cooling down to RT. The SU8 was developed in EC11 solvent for 1 min and then rinsed in IPA for 1 min. After drying in a nitrogen flow, the samples were hard-baked at 180 °C for 15 min to improve the mechanical properties of the SU8 and to promote the adhesion of the SU8 to the Au layer. The samples were cooled down to RT slowly before they were immersed into gold etchant (KI/I) and then a Ti etchant (NH_4OH:H_2O_2:H_2O = 1:1:5). After wet-etching, the samples were rinsed in deionized water and blow dried with nitrogen. The microchannels produced by this method were 5, 10 and 20 μm wide, all of which featured a 10-nm-thick Ti layer topped with a 500-nm-thick layer of Au and a 1000 nm SU8 atop the Au. The SU8 on the pad used to make the electrical connection (Figure 1b) was removed by O_2 plasma etching.

Filling of the Microchannels and Alignment of the DLC: A crystalline sample of the DLC was added at the edge of the microchannel region and the sample was heated on a Linkam TMS94 heated stage to one or two degrees above the Col/I phase transition temperature of the liquid crystal. The isotropic melt filled the microchannels by capillary action. The sample was then slowly cooled into the mesophase: usually at 0.1 °C/min.

Characterization by Polarizing Optical Microscopy (POM): A Leica DM LM microscope was used, with a halogen light source (12 V, 100 W) and a Canon 350 camera attached to the eyepiece of the microscope through a custom made stage. For samples on glass slides, images were recorded in transmission mode and for silicon wafers, in reflection mode.

Characterization by AFM: A silicon wafer with 2-μm-wide microchannels and SU8 barriers was filled with H7T which was aligned by slow cooling into the Colh phase. The resultant system was analyzed using Nanoman and Multimode instruments (Veeco). Measurements were made in a tapping mode at room temperature.

Conductivity: The *I–V* characteristics of the DLCs aligned between the interdigitated electrodes were acquired using a Keithley 6514 System Electrometer and Keithley 2400 Sourcemeter linked to a computer that allowed the voltage range and sweep rate to be varied. The temperature of the sample was controlled using a Linkam TMS91 heated stage. The electrical connections to the interdigitated electrodes were made through thin copper wires using silver paint and the wires were secured using Araldite to ensure a sturdy connection.

Supporting Information

Supporting Information is available from the Wiley Online Library or from the author.

Acknowledgements

We thank the Wolfson Foundation for partial funding of J.C. and the EPSRC for the funding of D.J.T. We also thank Dr Alex Walton for assistance with the electrochemical measurements.

Received: May 10, 2013
Published online: June 25, 2013

[1] K. Kawata, *Chem. Rec.* **2002**, *2*, 59–80.
[2] R. J. Bushby, K. Kawata, *Liq. Cryst.* **2011**, *38*, 1415–1426.
[3] D. Sharma, A. D. Rey, *Liq. Cryst.* **2003**, *30*, 377–389.
[4] S. Kundu, A. A. Ogale, *Rheol. Acta*. **2010**, *49*, 845–854.
[5] J. Yan, A. D. Rey, *Phys. Rev. E* **2002**, *65*, 031713.
[6] A. M. van de Craats, N. Stutzmann, O. Bunk, M. M. Nielsen, M. Watson, K. Mullen, H. D. Chanzy, H. Sirringhaus, R. H. Friend, *Adv. Mater.* **2003**, *15*, 495–499.
[7] R. J. Chesterfield, J. C. McKeen, C. R. Newman, P. C. Ewbank, D. A. da Silva, J. L. Bredas, L. L. Miller, K. R. Mann, C. D. Frisbie, *J. Phys. Chem. B* **2004**, *108*, 19281–19292.

[8] F. Nolde, W. Pisula, S. Muller, C. Kohl, K. Mullen, *Chem. Mater.* **2006**, *18*, 3715–3725.
[9] H. N. Tsao, W. Pisula, Z. H. Liu, W. Osikowicz, W. R. Salaneck, K. Mullen, *Adv. Mater.* **2008**, *20*, 2715–2719.
[10] S. X. Xiao, M. Myers, Q. Miao, S. Sanaur, K. Pang, M. L. Steigerwald, C. Nuckolls, *Angew. Chem. Int. Ed.* **2005**, *44*, 7390–7394.
[11] X. Guo, S. Xiao, M. Myers, Q. Miao, M. L. Steigerwald, C. Nuckolls, *Proc. Nat. Acad. Sci. USA* **2009**, *106*, 691–696.
[12] W. Pisula, A. Menon, M. Stepputat, I. Lieberwirth, U. Kolb, A. Tracz, H. Sirringhaus, Y. Pakula, K. Mullen, *Adv. Mater.* **2005**, *17*, 684–689.
[13] L. Schmidt-Mende, A. Fechtenkotter, K. Mullen, E. Moons, R. H. Friend, J. D. MacKenzie, *Science* **2001**, *293*, 1119–1122.
[14] L. Schmidt-Mende, A. Fechtenkotter, K. Mullen, R. H. Friend, J. D. MacKenzie, *Physica E* **2002**, *14*, 263–267.
[15] J. P. Schmidtke, R. H. Friend, M. Kastler, K. Mullen, *J. Chem. Phys.* **2006**, *124*, 174704.
[16] H. C. Hesse, J. Weickert, M. Al-Hussein, L. Dossel, X. L. Feng, K. Mullen, L. Schmidt-Mende, *Sol. Energy Mater. Sol. Cells* **2010**, *94*, 560–567.
[17] V. De Cupere, J. Tant, P. Viville, R. Lazzaroni, W. Osikowicz, W. R. Salaneck, Y. H. Geerts, *Langmuir* **2006**, *22*, 7798–7806.
[18] Z. H. Al-Lawati, R. J. Bushby, S. D. Evans *J. Phys. Chem. C* **2013**, *117*, 10702–1070.
[19] E. Grelet, H. Bock, *Europhys. Lett.* **2006**, *73*, 712–718.
[20] E. Charlet, E. Grelet, P. Brettes, H. Bock, H. Saadaoui, L. Cisse, P. Destreul, N. Gherardi, I. Seguy, *Appl. Phys. Lett.* **2008**, *92*, 024107.
[21] S. Xiao, M. Myers, Q. Miao, S. Sanaur, K. Pang, M. L. Steigerwald, C. Nuckolls, *Angew. Chem. Int. Ed.* **2005**, *44*, 7390–7394.
[22] G. Scherowsky, X. H. Chen, *J. Mater. Chem.* **1995**, *5*, 417–421.
[23] J. Piris, M. G. Debije, N. Stutzmann, B. W. Laursen, W. Pisula, M. D. Watson, T. Bjornholm, K. Mullen, J. M. Warman, *Adv. Funct. Mater.* **2004**, *14*, 1053–1061.
[24] J. C. Wittmann, P. Smith, *Nature* **1991**, *352*, 414–417.
[25] S. Zimmermann, J. H. Wendorff, C. Weder, *Chem. Mater.* **2002**, *14*, 2218–2223.
[26] A. M. van de Craats, N. Stutzmann, O. Bunk, M. M. Nielsen, M. Watson, K. Mullen, H. D. Chanzy, H. Sirringhaus, R. H. Friend, *Adv. Mater.* **2003**, *15*, 495–499.
[27] E. Charlet, E. Grelet, *Phys. Rev. E* **2008**, *78*, 041707.
[28] A. Tracz, J. K. Jeszka, M. D. Watson, W. Pisula, K. Mullen, T. Pakula, *J. Am. Chem. Soc.* **2003**, *125*, 1682–1683.
[29] M. Kastler, W. Pisula, D. Wasserfallen, T. Pakula, K. Mullen, *J. Am. Chem. Soc.* **2005**, *127*, 4286–4296.
[30] D. W. Breiby, O. Bunk, W. Pisula, T. I. Solling, A. Tracz, T. Pakula, K. Mullen, M. M. Nielsen, *J. Am. Chem. Soc.* **2005**, *127*, 11288–11293.
[31] D. W. Breiby, F. Hansteen, W. Pisula, O. Bunk, T. I. Solling, U. Kolb, J. W. Andreasen, K. Mullen, M. M. Nielsen, *J. Phys. Chem. B* **2005**, *109*, 22319–22325.
[32] C.-Y. Liu, A. J. Bard, *Chem. Mater.* **2000**, *12*, 2353–2362.
[33] P. O. Mouthuy, S. Melinte, Y. H. Geerts, A. M. Jonas, *Nano Lett.* **2007**, *7*, 2627–2632.
[34] P. O. Mouthuy, S. Melinte, Y. H. Geerts, B. Nysten, A. M. Jonas, *Small* **2008**, *4*, 728–732.
[35] J. P. Bramble, D. J. Tate, D. J. Revill, K. H. Sheikh, J. R. Henderson, F. Liu, X. B. Zeng, G. Ungar, R. J. Bushby, S. D. Evans, *Adv. Func. Mater.* **2010**, *20*, 914–920.
[36] R. Seemann, M. Brinkmann, E. J. Kramer, F. F. Lange, R. Lipowsky, *Proc. Nat. Acad. Sci. USA* **2005**, *102*, 1848–1852.
[37] K. Khare, S. Herminghaus, J. C. Barat, B. M. Law, M. Brinkmann, R. Seemann, *Langmuir* **2007**, *23*, 12997–13006.
[38] P. Oswald, P. Pieranski, *Smectic and Columnar Liquid Crystals*, Taylor and Frances, Boca Raton, **2006**.
[39] F. C. Frank, S. Chandrasekhar, *J. Physique* **1980**, *41*, 1285–1288.
[40] C. R. Safinya, N. A. Clark, K. S. Liang, W. A. Varady, L. Y. Chiang, *Mol. Cryst. Liq. Cryst.* **1985**, *123*, 205–216.
[41] A. S. Cherodian, A. N. Davies, R. M. Richardson, M. J Cook, N. B. McKeown, A. J. Thomson, J. Feijoo, G. Ungar, K. J. Harrison, *Mol. Cryst. Liq. Cryst.* **1991**, *196*, 103–114.
[42] J. Malthete, J. Jacques, N. H. Tinh, C. Destrade, *Nature* **1982**, *298*, 46–48.
[43] N. A. Clark, S. T. Lagerwall, *Appl. Phys. Lett* **1980**, *36*, 899–901.
[44] M. Hird, *Liq. Cryst.* **2011**, *38*, 1467–1493.
[45] H. Bock, W. Helfrich, *Liq. Cryst.* **1992**, *12*, 697–703.
[46] H. Bock, W. Helfrich, *Liq. Cryst.* **1995**, *18*, 387–399.
[47] D. Miyajima, K. Tashiro, F. Araoka, H. Takezoe, J. Kim, K. Kato, M. Takata, T. Aida, *J. Am. Chem. Soc.* **2009**, *131*, 44–45.
[48] D. Miyajiama, F. Araoka, H. Takezoe, J. Kim, K. Kato, M. Takata, *Angew. Chem. Int. Ed.* **2011**, *50*, 7865–7869.
[49] D. Miyajima, F. Araoka, H. Takezoe, J. Kim, K. Kato, M. Takata, T. Aida, *Science* **2012**, *336*, 209–213.
[50] H. Takezoe, K. Kishikawa, E. Gorecka, *J. Mater. Chem.* **2006**, *16*, 2412–2416.
[51] M. Prehm, F. Lui, U. Baumeister, X. Zeng, G. Ungar, C. Tschierske, *Angew. Chem. Int. Ed.* **2007**, *46*, 7972–7975.
[52] F. Lui, M. Prehm, X. Zeng, G. Ungar, C. Tschierske, *Angew. Chem. Int. Ed.* **2011**, *50*, 10599–10602.
[53] A. McNeill, R. J. Bushby, S. D. Evans, Q. Liu, B. Movaghar in *3D Nanoelectronic Computer Architecture and Implementation* (Eds: D. Crawley, K. Nikolic, M. Forshaw) Institute of Physics Publishing, Bristol, **2005**, pp. 203–233.
[54] S. Kumar, M. Manickam, S. K. Varshney, D. S. S. Rao, S. K. Prasad, *J. Mater. Chem.* **2000**, *10*, 2483–2489.
[55] N. Boden, R. C. Borner, R. J. Bushby, A. N. Cammidge, M. V. Jesudason, *Liq. Cryst.* **1993**, *15*, 851–858.
[56] Y. Maeda, D. S. S. Rao, S. K. Prasad, S. Chandrasekhar, S. Kumar, *Liq. Cryst.* **2001**, *28*, 1679–1690.
[57] H. Iino, J. Hanna, R. J. Bushby, B. Movaghar, B. J. Whitaker, M. J. Cook, *Appl. Phys. Lett.* **2005**, *87*, 132102.
[58] D. J. Tate, R. Anémian, R. J. Bushby, S. Nanan, S. L. Warriner, B. J. Whitaker, *Beilstein J. Org. Chem.* **2012**, *8*, 120–128.